mounted in a glass capillary under argon. Experimental details may be found in Table V.

Systematic absences observed, $0k0$, $k = 2n + 1$, are consistent with space groups $P2_1$ (No. 4) or $P2_1/m$ (No. 11). A Patterson synthesis allowed location of the tungsten atom; difference Fourier calculations allowed location of other atoms. The molecule is disordered in $P2_1/m$ in one-half of the molecule. Phosphine group P(1) is ordered and all carbon atoms in this ligand were located and refined anisotropically. Most hydrogen atoms were located from ΔF maps and were fixed in positions thus obtained; others were calculated. However, the data did not allow resolution of individual components of each disordered carbon atom, except in the case of atom C(9), which lies ~0.5 Å from the mirror plane at $y = {}^1/_4$, and was included with an "occupancy" factor of ${}^1/_2$. Electron density in the remaining "half-atoms" is described by artificially large thermal ellipsoids.

Since the disorder in $P2_1/m$ affected only a few atoms, we carried out final refinement in this space group. The model consisted of 119 parameters with 2212 data and resulted in $R_F = 0.033$ and $R_{wF} = 0.046$. The refined value of the mosaic block size (secondary extinction) parameter[29] was 1.14 (8) × 10^{-5} mm. Final positional parameters are listed in Table VII; thermal parameters may be found in Table IIIs.

Acknowledgment. This work was performed under the auspices of the U.S. Department of Energy, Division of Chemical Science, Office of Basic Energy Sciences.

Supplementary Material Available: Lists of analytical data (Table Is), anisotropic thermal parameters (Tables IIs and IIIs), and structure factor amplitudes (Table IVs and Vs) (28 pages). Ordering information is given on any current masthead page.

Formation and Cleavage of N–H Bonds on Nitrido Metal Carbonyl Clusters

Margaret L. Blohm,[1] Douglas E. Fjare, and Wayne L. Gladfelter*[2]

Contribution from the Department of Chemistry, University of Minnesota, Minneapolis, Minnesota 55455. *Received September 3, 1985*

Abstract: A study of the protonation of three tetranuclear nitrido clusters having the butterfly geometry is reported. While the final product of each of these reactions is a hydrido–nitrido cluster, the intermediates contain the imido (NH) ligand which can be trapped by CO. For $[FeRu_3N(CO)_{12}]^{1-}$, the products of protonation in a CO atmosphere are $FeRu_2(NH)(CO)_{10}$, $[FeRu_4N(CO)_{14}]^{1-}$, and small amounts of $HFeRu_3N(CO)_{12}$ and $Ru_3(CO)_{12}$. With $[Ru_4N(CO)_{12}]^{1-}$, this reaction generates $Ru_3(NH)(CO)_{10}$, $[Ru_5N(CO)_{14}]^{1-}$, $HRu_4N(CO)_{12}$, and small quantities of $Ru_3(CO)_{12}$. The new NH-containing clusters $FeRu_2(NH)(CO)_{10}$ and $Ru_3(NH)(CO)_{10}$ contain a triply bridging N–H ligand and a triply bridging carbon monoxide. The substituted cluster $\{FeRu_3N(CO)_{10}[P(OCH_3)_3]_2\}^{1-}$ was shown by X-ray crystallography [crystal system = orthorhombic, space group = *Pnn*2, $a = 11.603$ (3) Å, $b = 18.521$ (6) Å, $c = 8.908$ (4) Å, $Z = 2$] to contain the two $Ru(CO)_2[P(OCH_3)_3]$ fragments in the wing-tip positions. Protonation leads to a green intermediate that reacts with CO to give $FeRu_2(NH)(CO)_9[P(OCH_3)_3]$, which was structurally characterized [crystal system = monoclinic, space group = $P2_1/m$, $a = 8.596$ (2) Å, $b = 15.576$ (3) Å, $c = 7.870$ (4) Å, $\beta = 100.37$ (3)°, $Z = 2$]. The structure contains both a triply bridging CO and NH ligand, and the phosphite is bound to a ruthenium and oriented trans to the NH group. ^1H and ^{15}N NMR spectroscopies were used to identify the intermediate imido cluster $FeRu_3(NH)(CO)_{10}[P(OCH_3)_3]_2$.

The formation and cleavage of N–H bonds on metal surfaces is an integral part of several important heterogeneously catalyzed reactions such as the Haber process[3] and the oxidation of ammonia.[4] In some of these reactions, surface-coordinated nitrogen atoms are key intermediates. Much of the interest in metal carbonyl clusters containing a nitrido ligand stems from the comparison of their reactivity to those of nitrogen atoms bound to metal surfaces. We report in this paper the results of our studies of the protonation of several nitrido clusters in which the initially formed imido (NH) cluster undergoes a facile N–H bond cleaving reaction, yielding a hydrido–nitrido cluster.

Experimental Section

$PPN[Ru_4N(CO)_{12}]$,[5] $PPN[Ru_4{}^{15}N(CO)_{12}]$,[5] $PPN[FeRu_3N(CO)_{12}]$,[6] $PPN[FeRu_3{}^{15}N(CO)_{12}]$,[6] and $PPN\{FeRu_3N(CO)_{10}[P(OCH_3)_3]_2\}$[7] were prepared according to published procedures. Tetrahydrofuran (THF) and diethyl ether were distilled from sodium benzophenone ketyl under nitrogen. Hexane was dried by distillation from sodium metal under nitrogen. Methylene chloride was distilled from P_2O_5 immediately prior to use. All reactions were carried out under a nitrogen atmosphere, and chromatography was conducted on silica gel. Infrared spectra were recorded on a Beckman Model 4250 spectrophotometer or Mattson Cygnus 25 FTIR spectrophotometer equipped with a HgCdTe detector. NMR data were recorded on a Nicolet NTCFT-1130 300-MHz spectrophotometer. Each ^{15}N NMR experiment was conducted with CH_2Cl_2 as the solvent (3.0 mL) in a 12-mm tube with $Cr(acac)_3$ (53 mg) as the shiftless relaxation reagent. Nitromethane was used as an external reference, set at 379.60 ppm downfield from NH_3(liquid, 25 °C).[8] A summary of the spectroscopic data is shown in Table I.

$PPN[FeRu_3N(CO)_{12}] + CF_3SO_3H$. CH_2Cl_2 (10 mL) was distilled into a Schlenk tube containing 202.0 mg (0.162 mmol) of $PPN[FeRu_3N(CO)_{12}]$. CF_3SO_3H (16.5 μL, 0.165 mmol) was added by syringe, causing a deep-red color that lasted for several minutes. The solution was stirred for 10 min. After the solvent was removed, the product was extracted into 2 × 50 mL of hexane. The hexane was evaporated, leaving 109 mg (0.152 mmol, 95%) of amber crystalline $HFeRu_3N(CO)_{12}$. The product can be recrystallized by slowly cooling a saturated hexane solution. Anal. Calcd for $C_{12}HFeNO_{12}Ru_3$: C, 20.09; H, 0.14; N, 1.97. Found: C, 20.32; H, 0.15; N, 1.97.

$PPN[FeRu_3N(CO)_{12}] + CF_3SO_3H$ under CO. $PPN[FeRu_3N(CO)_{12}]$ (200 mg, 0.160 mmol) was dissolved in 10 mL of CH_2Cl_2, and the resulting solution was saturated with CO. Immediately following the addition of 14.3 μL of CF_3SO_3H (0.160 mmol), a dark-red color was observed for several seconds, after which a stable orange solution was formed. The volume of CH_2Cl_2 was reduced to ~1 mL and was extracted with 4 × 10 mL of hexane. After filtration of the yellow–orange hexane solution, the products were separated by column chromatography. When hexane was used as the eluent, four bands were observed. The first band to elute contained trace amounts of $Ru_3(CO)_{12}$ and was closely

(1) NSF Predoctoral Fellow, 1982–1985.
(2) Alfred, P. Sloan Fellow, 1983–1985.
(3) Czaka, A.; Aika, K. *Catal. Sci. Technol.* **1981**, *3*, 87.
(4) Pignet, T.; Schmidt, L. D. *J. Catal.* **1975**, *40*, 212.
(5) Blohm, M. L.; Gladfelter, W. L. *Organometallics* **1985**, *4*, 45.
(6) Fjare, D. E.; Gladfelter, W. L. *J. Am. Chem. Soc.* **1984**, *106*, 4799.
(7) Fjare, D. E. Ph.D. Dissertation, University of Minnesota, Minneapolis, 1983.
(8) Levy, G. C.; Lichter, R. L. "Nitrogen-15 Nuclear Magnetic Resonance Spectroscopy"; Wiley: New York, 1979.

0002-7863/86/1508-2301$01.50/0

Table I. Summary of Spectroscopic Data

compound	color	ν_{N-H}, cm^{-1} (CH_2Cl_2)	ν_{CO}, cm^{-1} (hexane)	^1H, ppm ($CDCl_3$)
$HFeRu_3N(CO)_{12}$	orange		2104 w, 2071 s, 2062 s, 2043 s, 2029 s, 2000 m, 1991 m, 1968 w, 1955 w	−24.52
$HFeRu_3N(CO)_{10}[P(OCH_3)_3]_2$	orange		2074 w, 2038 s, 2021 vs, 2009 s, 1933 m, 1978 m, 1961 m	3.78 (d, 9 H, $J_{^1H-^{31}P}$ = 12.6 Hz), 3.65 (d, 9 H, $J_{^1H-^{31}P}$ = 11.7 Hz), −23.92 (d of d, 1 H, $J_{^1H-^{31}P}$ = −24.13)
$HRu_4N(CO)_{12}$[17]	yellow		2068 vs, 2053 m, 2028 s, 1999 m	
$Ru_3(NH)(CO)_{10}$	yellow	3378	2104 vw, 2069 s, 2012 m, 1749 m	5.7 (t, 1 H, $J_{^1H-^{14}N}$ = 54 Hz)
$FeRu_2(NH)(CO)_{10}$	yellow	3372	2104 w, 2070 s, 2057 vs, 2029 s, 2023 m (sh), 2006 m, 1993 w, 1744 m	6.5 (t, 1 H, $J_{^1H-^{14}N}$ = 54 Hz)
$FeRu_2(NH)(CO)_9[P(OCH_3)_3]$	yellow	3374	2084 m, 2048 s, 2033 s, 2015 s, 2000 m, 1725 w, 1715 w	3.69 (d, 9 H, $J_{^1H-^{31}P}$ = 12.5 Hz), 6.7 (t, 1 H, $J_{^1H-^{14}N}$ = 43 Hz)

followed by $HFeRu_3N(CO)_{12}$ (20 mg, 15%). Separation of the next two very slow bands was difficult but yielded $Ru_3(NH)(CO)_{10}$ (2 mg, 4%) and yellow $FeRu_2(NH)(CO)_{10}$ (40.8 mg, 45%). Anal. Calcd for $C_{10}HFeO_{10}NRu_2$: C, 21.72; H, 0.18; N, 2.53. Found: C, 23.02; H, 0.77; N, 2.44. Extraction of the hexane insoluble residue with Et_2O led to the isolation of 26.5 mg $PPN[FeRu_4N(CO)_{14}]$.[6]

$PPN[Ru_4N(CO)_{12}] + CF_3SO_3H$. A volume of 5 mL of CH_2Cl_2 was distilled into a Schlenk tube containing 50.0 mg (0.378 mmol) of $PPN[Ru_4N(CO)_{12}]$. CF_3SO_3H (3.3 μL, 0.378 mmol) was added by syringe. The orange solution immediately turned deep purple, which lasted 2 h. After removal of the solvent under vacuum, the products were extracted into 3 × 10 mL of hexane, filtered, and chromatographed by using hexane as the eluent. Two bands eluted from the column; isolation of the first fraction gave yellow $HRu_4N(CO)_{12}$ (18.5 mg, 62%). Anal. Calcd for $C_{12}HNO_{12}Ru_4$: C, 19.08; H, 0.13; N, 1.85. Found: C, 19.32; H, 0.12; N, 1.86. The second band contained lemon-yellow $Ru_3(NH)(CO)_{10}$ (1.5 mg, 7%), characterized below.

$PPN[Ru_4N(CO)_{12}] + CF_3SO_3H$ under CO. A volume of 10 mL of CH_2Cl_2 was distilled into a Schlenk tube containing 81.7 mg (0.0618 mmol) of $PPN[Ru_4N(CO)_{12}]$. CO was bubbled through the solution for 10 min. CF_3SO_3H (5.5 μL, 0.0622 mmol) was added to the solution, resulting in a color change from orange to purple. After 5 min, the purple had disappeared, leaving a red solution. The volume was reduced to ~1 mL, 20 mL of hexane was added, and the solution was filtered. The insoluble residue was extracted with an additional 10 mL of hexane, and the hexane filtrates were combined and chromatographed by using hexane as the eluent. Three bands were seen on the column; $Ru_3(CO)_{12}$ was closely followed by $HRu_4N(CO)_{12}$ (4.8 mg, 10%), while collection of the third band led to the isolation of yellow crystalline $Ru_3(NH)(CO)_{10}$ (26.2 mg) in 71% yield. Anal. Calcd for $C_{10}HNO_{10}Ru_3$: C, 20.07; H, 0.16; N, 2.34. Found: C, 20.90; H, 0.52; N, 2.73. Mass spectrum, m/z 601 (parent). Extraction of the hexane insoluble solid with 2 × 10 mL of Et_2O, followed by filtration and layering of the filtrate with hexane, yielded 13.2 mg of $PPN[Ru_5N(CO)_{14}]$[5] (2% yield).

$PPN\{FeRu_3N(CO)_{10}[P(OCH_3)_3]_2\} + CF_3SO_3H$. $PPN\{FeRu_3N(CO)_{10}[P(OCH_3)_3]_2\}$ (198.0 mg, 0.138 mmol) was dissolved in 20 mL of CH_2Cl_2, and 12.2 μL of CF_3SO_3H (0.138 mmol) was added by syringe. An immediate color change occurred from orange to dark green. After stirring for 1 day at room temperature, the solution was orange. The volume was reduced to ~1 mL, and 10 mL of hexane was added. This solution was filtered, and the remaining residue was extracted with hexane until the extracts were colorless. The combined hexane filtrates were chromatographed by using a 3:7 CH_2Cl_2/hexane mixture as the eluent. Only one band eluted, and it contained 78.5 mg of $HFeRu_3N(CO)_{10}[P(OCH_3)_3]_2$ (63% yield). Anal. Calcd for $C_{16}H_{19}FeNO_{16}P_2Ru_3$: C, 21.30; H, 2.12; N, 1.55. Found: C, 21.32; H, 2.22; N, 1.60.

$PPN\{FeRu_3{}^{15}N(CO)_{10}[P(OCH_3)_3]_2\} + CF_3SO_3H$. $PPN\{FeRu_3{}^{15}N(CO)_{10}[P(OCH_3)_3]_2\}$ (30.0 mg, 0.0208 mmol) was placed in a 5-mm NMR tube, capped with a rubber septum, and purged with nitrogen. CD_2Cl_2 (0.6 mL) was added by syringe, followed by 1.9 μL (0.0210 mmol) of CF_3SO_3H. Immediately after addition of the acid, the NMR spectrum had very broad peaks with $\nu_{1/2} \sim 100$ Hz. After several minutes, the peaks sharpened to their normal line widths.

$PPN\{FeRu_3N(CO)_{10}[P(OCH_3)_3]_2\} + CF_3SO_3H$ under CO. CH_2Cl_2 (15 mL) was distilled into a Schlenk tube containing 130.9 mg (0.0909 mmol) of $PPN\{FeRu_3N(CO)_{10}[P(OCH_3)_3]_2\}$. CO was bubbled through the orange solution for 10 min before the addition of 8.0 μL (0.0909 mmol) of CF_3SO_3H. A dark-green color formed immediately, lasting 15 min until a stable orange color was observed. The volume of the solution was reduced to ~1 mL, and the resulting oil was extracted with 3 × 10 mL of hexane. After filtering the combined hexane extracts, the yellow–orange solution was chromatographed by using a 7:3 hexane/CH_2Cl_2 mixture as the eluting solvent. Four products were isolated; the first two fractions contained trace amounts of $Ru_3(CO)_{12}$ and $HFeRu_3N(CO)_{11}[P(OCH_3)_3]$,[7] respectively. The third fraction was $HFeRu_3N(CO)_{10}[P(OCH_3)_3]_2$ (8.2 mg, 11%), while the fourth band contained the major product, $FeRu_2(NH)(CO)_9[P(OCH_3)_3]$ (24.2 mg, 41%). Anal. Calcd for $C_{12}H_{10}FeNO_{12}PRu_2$: C, 24.59; H, 1.72; N, 2.39. Found: C, 24.68; H, 1.74; N, 2.05.

Collection and Reduction of the X-ray Data. $Et_4N\{FeRu_3N(CO)_{10}[P(OCH_3)_3]_2\}$. Red crystals were grown by slow diffusion of hexane into a CH_2Cl_2 solution of the cluster. A suitable, approximately equidimensional (0.2 mm) crystal was chosen and mounted on a glass fiber. The crystal was found to be orthorhombic by the Enraf-Nonius CAD4-SDP peak search, centering, and indexing programs and by a Delaunay reduction calculation.[9] The systematic absences at ($0kl$, $k+l = 2n + 1$; $h0l$, $h+l = 2n + 1$) were consistent with either *Pnn*2 or *Pnnm*. *Pnn*2 was chosen which requires the cluster to lie on a 2-fold symmetry site. A summary of the crystal and intensity measurement parameters is presented in Table II. Background counts were measured at both ends of the $\omega - 2\theta$ scan, equal at each side to one-fourth of the scan range of the peak. In this manner, the total duration of the measuring background is equal to half of the time required for the peak scan. The check reflections showed no significant decay throughout the entire data collection. The data were corrected for Lorentz, polarization, and background effects but not for absorption.[10] The crystal was inadvertently lost prior to the collection of the ψ-scan data.

$FeRu_2(NH)(CO)_9[P(OCH_3)_3]$. A red crystal with dimensions 0.05 × 0.2 × 0.2 mm was chosen and mounted on a glass fiber. The crystal was found to be monoclinic by the Enraf-Nonius CAD4-SDP peak search, centering, and indexing programs and by a Delaunay reduction calculation.[9] The systematic absences ($0k0$, $k = 2n + 1$) indicated either the centric space group $P2_1/m$ or the acentric space group $P2_1$. The centric group was chosen, and data collection was begun. The successful solution of the structure verified this choice. The crystal and intensity measurement parameters are listed in Table II. The background was measured in the same fashion as described for $Et_4N\{FeRu_3N(CO)_{10}[P(OCH_3)_3]_2\}$. The check reflections indicated no decay throughout the entire data collection. The data were corrected for Lorentz, polarization, background, and absorption effects.[10]

Solution and Refinement of the Structures. $Et_4N\{FeRu_3N(CO)_{10}[P(OCH_3)_3]_2\}$. The structure was solved by conventional heavy-atom techniques. The positions of the two unique metals (both labeled as Ru)

(9) All calculations were carried out on PDP 8A and 11/34 computers using the Enraf-Nonius CAD 4-SDP programs. This crystallographic computing package is described in: Frenz, B. A. In "Computing in Crystallography"; Schenk, H., Olthof-Hazekamp, R., van Koningsveld, H., Bassi, G. C., Eds.; Delft University Press: Delft, Holland, 1978; pp 64–71. See also: "CAD4 and SDP User's Manual"; Enraf-Nonius: Delft, Holland, 1978.

(10) The intensity data were processed as described: "CAD 4 and SDP User's Manual"; Enraf-Nonius: Delft, Holland, 1978. The net intensity $I = (K/NPI)(C - 2B)$, where $K = 20.116$(attenuator factor), NPI = ratio of fastest possible scan rate to scan rate for the measurement, C = total count, and B = total background count. The standard deviation in the net intensity is given by $\sigma^2(I) = (K/NPI)^2[C + 4B + (pI)^2]$, where p is a factor used to downweight intense reflections. The observed structure factor amplitude F_0 is given by $F_3 = (I/Lp)^{1/2}$, where Lp = Lorentz and polarization factors. The $\sigma(I)$'s were converted to the estimated errors in the relative structure factors $\sigma(R_0)$ by $\sigma(R_0) = {}^1/_2(\sigma(I)/I)F_0$.

Table II. Summary of Crystallographic Data

	$(Et_4N)\{FeRu_3N(CO)_{10}[P(OCH_3)_3]_2\}$	$FeRu_2(NH)(CO)_9[P(OCH_3)_3]$
	Crystal Parameters	
cryst system	orthorhombic	monoclinic
space group	*Pnn*2	$P2_{1/m}$
a, Å	11.603 (3)	8.596 (2)
b, Å	18.521 (6)	15.576 (3)
c, Å	8.908 (4)	7.870 (4)
β, deg	90	100.37 (3)
V, Å^3	1914 (2)	1036 (1)
Z	2	2
d(calcd), g cm^{-3}	1.817	2.077
temp, °C	22	22
abs coeff, cm^{-1}	16.677	22.352
	Measurement of Intensity Data	
diffractometer	Enraf-Nonius CAD4	Enraf-Nonius CAD4
radiation	Mo Kα (λ = 0.710 73 Å)	Mo Kα (λ = 0.710 73 Å)
monochromator	graphite crystal	graphite crystal
scan type	$\omega - 2\theta$	$\omega - 2\theta$
scan speed (variable from), deg/min	2.38–6.67	0.48–20.0
scan range, deg	$0 \le 2\theta \le 50$	$0 \le 2\theta \le 50$
reflcns measd	$+h,+k,+l$	$+h,+k,\pm l$
check reflcns	(800) (0,10,0), (174) measd approximately every 100 reflcns	(400), ($\bar{2}4\bar{1}$), (270) measd approximately every 100 reflcns
reflcns collected	2964 unique reflcns; 1410 with $I > 1.0\sigma(I)$	1681 unique reflcns; 1092 with $I > 1.0\sigma(I)$
p	0.05	0.04
R	0.059	0.030
R_w	0.060	0.033
error in observn of unit wt	1.408	1.081

Table III. Positional Parameters for $(Et_4N)\{FeRu_3N(CO)_{10}[P(OCH_3)_3]_2\}$

atom	*X*	*Y*	*Z*
Ru1	−0.006 45 (9)	0.104 63 (5)	0.0000 (0)
M2	0.112 1 (2)	0.003 7 (1)	0.1594 (3)
P	0.133 8 (4)	0.150 9 (2)	−0.1473 (5)
O1	0.196 1 (8)	0.098 9 (5)	−0.265 (1)
O2	0.260 8 (10)	0.172 7 (6)	−0.077 (1)
O3	0.086 4 (10)	0.215 4 (6)	−0.241 (1)
O4	−0.025 4 (12)	0.237 2 (8)	0.198 (2)
O5	−0.195 2 (10)	0.149 5 (7)	−0.209 (2)
O6	0.170 0 (10)	0.131 3 (7)	0.336 (2)
O7	0.343 2 (13)	−0.012 2 (6)	0.021 (2)
O8	0.1449 (11)	−0.103 8 (7)	0.403 (2)
N	0.000 0 (0)	0.000 0 (0)	−0.015 (2)
N2	0.000 0 (0)	0.500 0 (0)	0.049 (2)
C1	0.125 (1)	0.045 2 (8)	−0.342 (2)
C2	0.269 (2)	0.223 6 (11)	0.023 (2)
C3	0.157 (2)	0.251 0 (11)	−0.356 (3)
C4	−0.018 (1)	0.187 2 (10)	0.114 (2)
C5	−0.124 (1)	0.134 7 (9)	−0.121 (2)
C6	0.145 (1)	0.081 7 (8)	0.264 (2)
C7	0.249 (1)	−0.008 7 (8)	0.073 (2)
C8	0.130 (1)	−0.063 8 (9)	0.309 (2)
C1N	0.081 (2)	0.545 7 (10)	−0.051 (2)
C2N	0.018 (2)	0.595 8 (12)	−0.149 (3)
C3N	0.079 (1)	0.454 5 (9)	0.140 (2)
C4N	0.010 (1)	0.405 5 (10)	0.253 (2)

were located by a Patterson synthesis. After several cycles of alternating least-squares refinement with Fourier and difference Fourier calculations, all atoms were located. The temperature factors of the metals indicated that the iron is located only in the hinge position. Since the two hinge metals are equivalent by crystal symmetry, a model with a 50/50 occupancy of Fe and Ru was used. The positional and thermal parameters of the Fe were not independently refined but were tied to the values of the ruthenium. Idealized positions for the hydrogen atoms were added to the list but not refined. The limited data set allowed anisotropic refinement for only the metal atoms.[11] The final difference Fourier map revealed no features greater than 0.4 e/Å^3. The values of the atomic scattering factors used in the calculations were taken from the usual tabulation, and the effects of anomalous dispersion were included for the non-hydrogen atoms.[12,13] The positional parameters, bond distances, and bond angles are listed in Tables III, IV, and V.

Table IV. Interatomic Distances for $(Et_4N)\{FeRu_3N(CO)_{10}[P(OCH_3)_3]_2\}$

atoms	distance, Å	atoms	distance, Å
	A. Within $FeRu_3N$ Core		
Ru1–Ru1′	3.878 (2)	Ru1–N	1.944 (1)
Ru1–M2	2.721 (2)	M2–M2′	2.605 (4)
Ru1–M2′	2.746 (2)	M2–N	2.03 (1)
	B. Metal–Ligand Distances		
Ru1–C4	1.84 (2)	M2–C6	1.76 (2)
Ru1–C5	1.82 (2)	M2–C7	1.78 (2)
Ru1–P	2.259 (4)	M2–C8	1.84 (2)
	C. Ligand Distances		
C4–O4	1.20 (2)	P–O1	1.60 (1)
C5–O5	1.17 (2)	P–O2	1.65 (1)
C6–O6	1.16 (2)	P–O3	1.56 (1)
C7–O7	1.19 (2)	O1–C1	1.47 (1)
C8–O8	1.13 (2)	O2–C2	1.30 (2)
		O3–C3	1.47 (2)
	D. Cation Distances		
N2–C1N	1.55 (2)	C1N–C2N	1.47 (3)
N2–C3N	1.48 (2)	C3N–C4N	1.57 (2)

Table V. Selected Bond Angles for $(Et_4N)\{FeRu_3N(CO)_{10}[P(OCH_3)_3]_2\}$

atoms	angle, deg	atoms	angle, deg
	A. Within $FeRu_3N$ Core		
Ru–N–Ru1′	172.0 (4)	Ru1–M2–Ru1′	90.37 (8)
Ru1–N–M2	86.4 (2)	Ru1–M2–M2′	61.06 (8)
Ru1–N–M2′	87.4 (2)	M2–Ru1–M2′	56.90 (8)
M2–N–M2′	79.9 (2)		
	B. To Terminal Ligands		
M2–Ru1–C5	153.6 (3)	Ru1–M2–C6	79.6 (3)
M2–Ru1–C4	108.7 (3)	Ru1–M2–C7	108.3 (3)
M2–Ru1–P	101.5 (2)	Ru1–M2–C8	154.6 (3)
M2′–Ru1–C5	101.2 (3)	Ru1′–M2–C6	165.7 (3)
M2′–Ru1–P	154.0 (2)	Ru1′–M2–C7	94.6 (3)
M2′–Ru1–C4	106.9 (3)	Ru1′–M2–C8	85.9 (3)
N–Ru1–P	108.0 (3)	N–M2–C6	124.7 (6)
N–Ru1–C4	150.5 (7)	N–M2–C7	103.6 (6)
N–Ru1–C5	107.0 (7)	N–M2–C8	127.3 (6)
	C. Metal–Ligand–Ligand		
Ru1–P–O1	118.7 (4)	Ru1–C5–O5	172 (2)
Ru1–P–O2	121.0 (5)	M2–C6–O6	177 (1)
Ru1–P–O3	110.3 (5)	M2–C7–O7	175 (1)
Ru1–C4–O4	174 (2)	M2–C8–O8	177 (1)
	D. Phosphite and Cation		
P–O1–C1	117.6 (9)	C1N–N2–C3N′	112 (1)
P–O2–C2	120 (1)	C1N–N2–C1N′	110 (2)
P–O3–C3	122 (1)	N2–C1N–C2N	113 (1)
C1N–N2–C3N	104 (1)	N2–C3N–C4N	111 (1)

$FeRu_2(NH)(CO)_9[P(OCH_3)_3]$. The structure was solved by conventional heavy-atom techniques. The positions of the two unique metal atoms were located by a Patterson synthesis and both initially labeled as ruthenium. After several consecutive cycles of least-square refinement and difference Fourier calculations, all remaining non-hydrogen atoms were located. The thermal parameters for the metal labeled Ru1 indi-

(11) The function minimized was $\sum w(|F_o| - |F_o|)^2$, where $w = 1/\sigma^2(F_o)$. The unweighted and weighted residuals are defined as $R = (\sum||F_o| - |F_c||)/\sum|F_o|$ and $R_w = [(\sum w(|F_o| - |F_c|)^2/(\sum w|F_o|)^2]^{1/2}$. The error in an observation of unit weight is $[\sum w(|F_o| - |F_c|)^2/(NO - NV)]^{1/2}$, where NO and NV are the number of observations and variables, respectively.

(12) Cromer, D. T.; Waber, J. T. "International Tables for X-ray Crystallography"; Kynoch Press: Birmingham, England, 1974; Vol. IV, Table 2.2A. Cromer D. T., Table 2.3.1.

(13) Cromer, D. T.; Ibers, J. A. "International Tables for X-ray Crystallography"; Kynoch Press, Birmingham, England, 1974; Vol. IV, Table 2.2C.

Table VI. Positional Parameters for $FeRu_2(NH)(CO)_9[P(OCH_3)_3]$

atom	X	Y	Z
M1	0.118 50 (7)	0.164 72 (4)	0.280 24 (7)
Ru2	0.371 05 (8)	0.250	0.195 21 (8)
P	0.422 6 (3)	0.250	−0.080 9 (3)
N	0.263 6 (7)	0.250	0.404 9 (8)
C1	0.123 0 (9)	0.250	0.072 (1)
O1	0.059 5 (7)	0.250	−0.076 3 (7)
C11	0.239 3 (8)	0.067 8 (5)	0.327 8 (9)
O11	0.314 5 (7)	0.007 6 (3)	0.361 8 (8)
C12	−0.031 0 (8)	0.108 1 (4)	0.120 8 (9)
O12	−0.125 1 (6)	0.075 3 (4)	0.022 2 (7)
C13	0.001 9 (9)	0.152 8 (6)	0.453 9 (9)
O13	−0.062 5 (7)	0.141 4 (5)	0.565 4 (7)
C21	0.523 8 (8)	0.162 7 (4)	0.251 4 (7)
O21	0.618 9 (6)	0.112 3 (3)	0.288 6 (6)
O22	0.354 3 (5)	0.176 3 (3)	−0.211 8 (5)
C22	0.348 (1)	0.090 7 (5)	−0.165 (1)
O23	0.606 1 (7)	0.250	−0.078 4 (7)
C23	0.670 (1)	0.250	−0.235 (1)
H	0.332 0	0.250	0.500
H22A	0.305 9	0.053 0	−0.257 0
H22B	0.455 4	0.067 6	−0.117 0
H22C	0.288 6	0.081 3	−0.072 4
H23A	0.780 8	0.250	−0.214 1
H23B	0.632 6	0.200 2	−0.304 7

Table VII. Interatomic Distances for $FeRu_2(NH)(CO)_9[P(OCH_3)_3]$

atoms	distance, Å	atoms	distance, Å
A. Within $FeRu_2(NH)(CO)$ Core			
M1–M1′	2.657 (1)	M1–C1	2.116 (7)
M1–Ru2	2.729 (1)	Ru2–C1	2.178 (9)
M1–N	1.960 (5)	N–H	0.865 (6)
Ru2–N	2.031 (6)	C1–O1	1.20 (1)
B. Metal–Ligand Distances			
M1–C11	1.833 (9)	Ru2–C21	1.886 (7)
M1–C12	1.851 (8)	Ru2–P	2.295 (2)
M1–C13	1.844 (8)		
C. Ligand Distances			
C11–O11	1.143 (8)	P–O22	1.583 (4)
C12–O12	1.136 (8)	P–O23	1.574 (6)
C13–O13	1.133 (8)	O23–C23	1.44 (1)
C21–O21	1.134 (7)	O22–C22	1.387 (9)

cated that the iron was disordered in this site. A 50/50 Fe/Ru population of M1 and M1′ was approximated by using a multiplicity of 0.795 for Ru1. The hydrogen atoms were located on a difference Fourier map and were added to the list but not refined. All other atoms were treated anisotropically,[11] and the final difference Fourier map indicated no significant features. The values of the atomic scattering factors used in the calculations are taken from the usual tabulation,[12,13] and the effects of anomalous dispersion were included for the non-hydrogen atoms. The positional parameters, bond distances, and bond angles are listed in Tables VI, VII, and VIII.

Results and Discussion

Structure of $\{FeRu_3N(CO)_{10}[P(OCH_3)_3]_2\}^{1-}$. The structure consists of well-separated cations and anions. Since the basic structure of this cluster is similar (Figure 1) to other tetrametal nitrides,[6,14-19] the following comments will concentrate on the features pertinent to this study. The wing-tip positions are occupied by the $Ru(CO)_2[P(OCH_3)_3]$ groups related to each other by a crystallographic 2-fold axis. The phosphites are located in the sterically most unencumbered position in the anion, similar

Table VIII. Selected Bond Angles for $FeRu_2(NH)(CO)_9[P(OCH_3)_3]$

atoms	angle, deg	atoms	angle, deg
A. Within $FeRu_2(NH)(CO)$ Core			
M1–M1′–Ru2	60.88 (1)	M1–N–M1′	85.3 (3)
M1–M1′–N	47.3 (1)	M1–N–Ru2	86.3 (2)
M1–M1′–C1	51.1 (2)	M1–N–H	134.9 (2)
Ru2–M1′–N	48.0 (2)	Ru2–N–H	111.4 (5)
Ru2–M1′–C1	51.6 (2)	M1–C1–M1′	77.8 (3)
N–M1′–C1	82.2 (3)	M1–C1–Ru2	78.9 (3)
M1–Ru2–M1′	58.25 (3)	M1–C1–O1	133.4 (4)
M1–Ru–N	45.8 (1)	Ru2–C1–O1	132.3 (6)
M1–Ru2–C1	49.5 (2)		
N–Ru2–C1	79.1 (3)		
B. To Terminal Ligands			
M1′–M1–C11	145.5 (2)	C1–M1–C11	125.9 (3)
M1′–M1–C12	118.5 (2)	C1–M1–C12	83.2 (3)
M1′–M1–C13	95.8 (3)	C1–M1–C13	136.5 (4)
Ru2–M1–C11	90.3 (2)	M1–Ru2–P	122.0 (5)
Ru2–M1–C12	123.5 (2)	M1–Ru2–C21	98.2 (2)
Ru2–M1–C13	142.5 (2)	N–Ru2–P	164.4 (2)
N–M1–C11	99.8 (3)	N–Ru2–C21	102.1 (2)
N–M1–C12	164.6 (3)	C1–Ru2–P	88.7 (2)
N–M1–C13	94.5 (3)	C1–Ru2–C21	133.5 (2)
C11–M1–C12	92.6 (3)	P–Ru2–C21	88.7 (2)
C11–M1–C13	97.4 (4)	C21–Ru2–C21′	92.2 (4)
C12–M1–C13	92.9 (3)		
C. Within Terminal Ligands			
M1–C11–O11	178.2 (7)		
M1–C12–O12	178.2 (7)	O22–P–O22′	93.0 (3)
M1–C13–O13	175 (1)	O22–P–O23	105.2 (2)
Ru2–C21–O21	177.6 (6)	P–O22–C22	123.5 (4)
Ru2–P–O22	120.3 (2)	P–O23–C23	121.9 (6)
Ru2–P–O23	110.6 (2)		

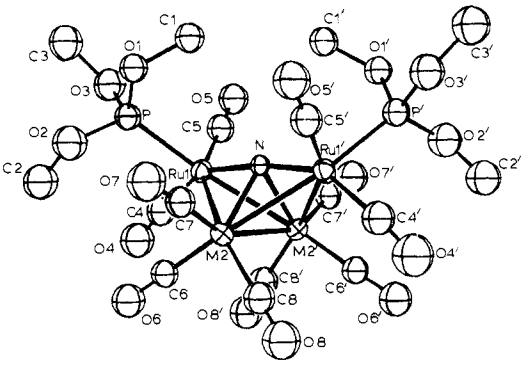

Figure 1. View of the anion in $(Et_4N)\{FeRu_3N(CO)_{10}[P(OCH_3)_3]_2\}$.

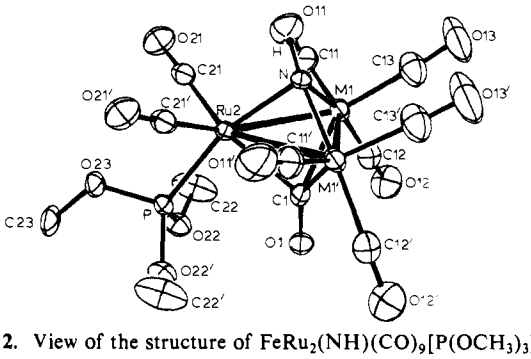

Figure 2. View of the structure of $FeRu_2(NH)(CO)_9[P(OCH_3)_3]$.

to the $P(OCH_3)_3$ position found in the structure of $HRu_4N(CO)_{11}[P(OCH_3)_3]$.[17] The remaining iron and ruthenium atoms are disordered between the two hinge sites of the cluster. The bulk of the phosphite ligands causes two distortions relative to the structure of $[FeRu_3N(CO)_{12}]$.[1-6] The hinge $M(CO)_3$ groups have twisted to reduce nonbonded repulsions between C7–O7 and the phosphite. One measure of this can be seen in the comparison of the angle Ru1–M2–C6 of 79.9 (6)° to Ru1′–M2–C8 of 85.9 (7)°. The dihedral angle between the planes comprised of

(14) Tachikawa, M.; Stein, J.; Muetterties, E. L.; Teller, R. G.; Beno, M. A.; Gebert, E.; Williams, J. M. *J. Am. Chem. Soc.* **1980**, *102*, 6648.
(15) Fjare, D. E.; Gladfelter, W. L. *Inorg. Chem.* **1981**, *20*, 3533.
(16) Collins, M. A.; Johnson, B. F. G.; Lewis, J.; Mace, J. M.; Morris, J.; McPartlin, M.; Nelson, W. J. H.; Puga, J.; Raithby, P. R. *J. Chem. Soc., Chem. Commun.* **1983**, 689.
(17) Braga, M.; Johnson, B. F. G.; Lewis, J.; Mace, J. M.; McPartlin, M.; Puga, J.; Nelson, W. J. H.; Raithby, P. R.; Whitmore, K. H. *J. Chem. Soc., Chem. Commun.* **1982**, 1081.
(18) Blohm, M. L.; Gladfelter, W. L., unpublished results.
(19) Fjare, D. E.; Gladfelter, W. L., unpublished results.

Ru1–M2–M2′ and Ru1′–M2–M2′ is 107.6°, which is wider than the value of 101.1° found in $[FeRu_3N(CO)_{12}]^{1-}$. Since the wings of the butterfly are slightly unfolded here relative to $[FeRu_3N(CO)_{12}]^{1-}$, the Ru1–N–Ru1′ angle has decreased to 172.0 (1)° in $\{FeRu_3N(CO)_{10}[P(OCH_3)_3]_2\}^{1-}$ compared to 176.6 (2°) in the unsubstituted structure.

Structure of $FeRu_2(NH)(CO)_9[P(OCH_3)_3]$. The cluster resides on a crystallographic mirror plane, with the atoms H–N–Ru2–C1–O1–P–O23–C23 lying in the plane. The structure, shown in Figure 2, contains three electronically equivalent ML_3 groups in a triangle which is capped by a μ_3-NH on one side and a μ_3-CO on the other. The phosphite is bound to Ru2, and the remaining ruthenium and the iron atoms are fully disordered at the M1 site, as required by the crystal symmetry. Neglecting the M–M vectors, each of the metals is surrounded by a trigonal-bipyramidal arrangement of ligands. The greatest deviation from this geometry is the C(equatorial)–M–C(equatorial) angle. Viewing each of the metals as having a trigonal-bipyramidal geometry highlights some useful observations that extend to several related structures.[20-23] We note that the μ_3-CO always exists in the equatorial plane, and the $4e^-$ donor (NH, NR,[20,23] NOR,[21] or S[22]) always resides in the axial position. In mononuclear five-coordinate complexes, the proclivity of the stronger donor ligand to coordinate in an axial position is well-established. Consistent with this treatment, the phosphite replaces the CO that was also in the axial position.

The N of the N–H ligand is symmetrically bridging the triangle when appropriate consideration is given to the different radii of Fe and Ru. The M–N–H angles differ significantly from each other with M1–N–H at 134.9 (2)° and Ru2–N–H at 111.4 (5)°. The cause of this bending is probably the close intermolecular contact between H and the phosphite on an adjacent cluster. Specifically, we note the intermolecular O22–H distance of 2.518 (4) Å and the H23B–H distance of 2.87 Å.

Formation of HM_4N from M_4N^-. The protonation of anionic clusters is often a straightforward route to hydrido clusters.[24] Not surprisingly, the ultimate hydrido products are usually obtained in good to nearly quantitative yields. Such is the case for the protonations of the three anionic nitrido clusters below, eq 1–3.

$$PPN[Ru_4N(CO)_{12}] + CF_3SO_3H \rightarrow HRu_4N(CO)_{12} \quad (1)$$

$$PPN[FeRu_3N(CO)_{12}] + CF_3SO_3H \rightarrow HFeRu_3N(CO)_{12} \quad (2)$$

$$PPN\{FeRu_3N(CO)_{10}[P(OCH_3)_3]_2\} + CF_3SO_3H \rightarrow HFeRu_3N(CO)_{10}[P(OCH_3)_3]_2 \quad (3)$$

The unusual feature common to each of these reactions is that they proceed through an intensely colored intermediate. The lifetime and color of the intermediate are dependent upon both the metal and ligands on the cluster.

Addition of CF_3SO_3H to an orange CH_2Cl_2 solution of $[Ru_4N(CO)_{12}]^{1-}$ results in the immediate formation of an intense purple that lasts for 2 h before the neutral yellow $HRu_4N(CO)_{12}$, **1** is isolated in 62% yield. This neutral cluster had been isolated

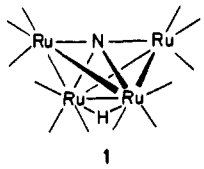

1

in low yield from the reaction of NO^+ with $[H_3Ru_4(CO)_{12}]^{1-}$ and structurally characterized as its trimethyl phosphite derivative, $HRu_4N(CO)_{11}[P(OCH_3)_3]$.[17] As in other neutral HM_4NL_{12} 62-electron clusters, the hydride bridges the hinge metal–metal bond of the butterfly core.[14,17]

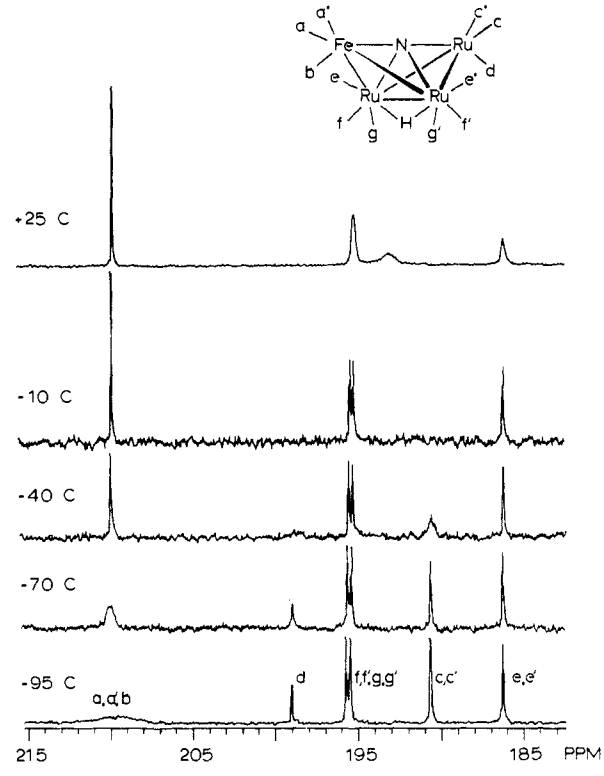

Figure 3. Variable-temperature $^{13}C\{^1H\}$ NMR spectrum of $HFeRu_3N(CO)_{12}$.

The structure of the anionic nitrido cluster $[FeRu_3N(CO)_{12}]^{1-}$ was recently determined[6] to consist of a butterfly metal core geometry similar to $[Fe_4N(CO)_{12}]^{1-}$,[15] $[Ru_4N(CO)_{12}]^{1-}$,[18] and $[Os_4N(CO)_{12}]^{1-}$.[16] The mixed-metal cluster, however, exists in two isomeric forms; in one isomer, the iron atom is located in the hinge position, **2**, while in the second isomer, **3**, the iron atom is located in the wing-tip position. Isomers **2** and **3** undergo a slow intramolecular isomerization with a half-life of several days at room temperature. When a mixture of the isomers is protonated, the orange–red solution turns to an extremely dark-red, which subsides after a few minutes to give the amber $HFeRu_3N(CO)_{12}$, **4**.

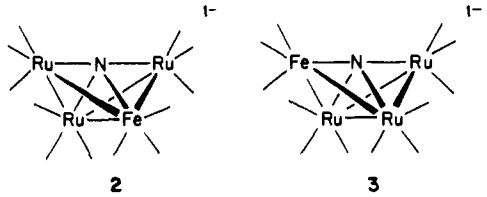

2 **3**

The infrared spectrum has absorptions due only to terminal carbonyls. Singlets were observed in both the ^1H and ^{15}N NMR at −24.52 and 530.0 ppm, respectively. The above spectroscopic

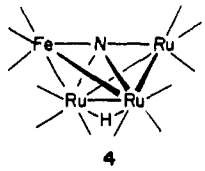

4

information suggests that the metal core still exists in the 62-electron butterfly geometry, with the hydride bridging a hinge M–M bond. Further, the appearance of singlets in both the ^1H and ^{15}N NMR spectra implies the existence of only one isomer.

Comparison of the location of the hydride resonance at −24.52 ppm with the hydride peak at −24.33 ppm reported[17] for $HRu_4N(CO)_{12}$ supports structure **4**, where the hydride is bridging a hinge Ru–Ru bond. If the hydrogen was bridging a Fe–Ru bond, the signal would be closer to that reported for $HFe_4N(CO)_{12}$ (−31.2 ppm).[14] The assignment of the structure of this isomer,

(20) Barnett, B.; Krüger, C. *Angew. Chem., Int. Ed. Engl.* **1971**, *10*, 910.
(21) Stevens, R. E.; Gladfelter, W. L. *J. Am. Chem. Soc.*, **1982**, *104*, 6454.
(22) Adams, R. D.; Horvēth, I. T.; Kim, H. S. *Organometallics* **1984**, *3*, 548.
(23) Bhaduri, S.; Gopalkrishnan, K. S.; Sheldrick, G. M.; Clegg, W.; Stalke, D. *J. Chem. Soc., Dalton Trans.* **1983**, 2339.
(24) Humphries, A. P.; Kaesz, H. D. *Prog. Inorg. Chem.* **1979**, *25*, 145.

specifically the location of the iron atom, can be unambiguously made from the low-temperature ^{13}C NMR spectra of $HFeRu_3N(CO)_{12}$ (Figure 3). At −95 °C, the coldest temperature measured, the $^{13}C\{^1H\}$ spectrum consists of a broad peak centered at ~210 ppm and five sharp peaks between 200 and 185 ppm in a 1:2:2:2:2 ratio. Since iron carbonyls are typically found downfield from ruthenium carbonyls, the five upfield peaks are assigned to the nine ruthenium carbonyls. The broad peak at 210 ppm is assigned to the iron tricarbonyl group, which is near its coalescence temperature. When the hydrogen is allowed to couple with the carbonyls, the peak farthest upfield at 186.3 ppm splits into a doublet ($J_{^{13}C-^1H}$ = 13 Hz). This peak is assigned to two equivalent carbonyls bound to ruthenium and located trans to the hydride bridging the hinge bond. The only cluster core geometry which accommodates this coupling is one where iron is located in the wing-tip position and the hydrogen is bridging the hinge ruthenium–ruthenium bond.[25]

A question remains, however, concerning the mechanism of the formation of a single isomer from the initial mixture of isomeric $[FeRu_3N(CO)_{12}]^{1-}$. The anion does not rearrange on a time scale sufficient to account for the observed isomeric specificity of the protonation, and the hydride, once formed, does not isomerize. A possible pathway responsible for the selectivity will be suggested below.

During the protonation of $\{FeRu_3N(CO)_{10}[P(OCH_3)_3]_2\}^{1-}$, **5**, an extremely dark-colored intermediate was observed, as was the case for both $[Ru_4N(CO)_{12}]^{1-}$ and $[FeRu_3N(CO)_{12}]^{1-}$. The dark-green solution lasted for 24 h before it was converted to an orange solution of $HFeRu_3N(CO)_{10}[P(OCH_3)_3]_2$, 6. Although the possibility for several isomers of the final product exists, spectroscopic evidence indicates that only one isomer is formed.

The crystal structure of the anion **5** locates the iron atom in the hinge position, with the wing-tip ruthenium atoms each substituted with one trimethyl phosphite ligand. In the hydride region of the ^1H NMR spectrum, the final product of protonation has a doublet of doublets ($J_{^{31}P-^1H}$ = 8.5 and 1.4 Hz) at −23.92 ppm. We concluded, as discussed above, that a chemical shift of −23.94 ppm suggests that the hydride is bridging a Ru–Ru hinge bond. The spectrum indicates that the hydride is coupled to two nonequivalent phosphites; the larger 8.5-Hz coupling constant can be assigned to a phosphite bound to a hinge ruthenium atom in a position cis to the bridging hydride.[24] The much smaller 1.5-Hz splitting is attributed to the coupling with a phosphite bound to a wing-tip metal atom. Three peaks are observed in the ^{31}P NMR spectrum; a broad peak occurs at 152.6 ppm, and two sharp peaks are found at 147.7 and 147.8 ppm. All these chemical shifts are consistent with trimethyl phosphite bound to ruthenium. Integration of the spectrum gives a 1:1 ratio between the broad lower field peak and the sum of the two sharp peaks. We attribute the complexity of the pattern to the different, but nearly equivalent, positions on both wing-tip and hinge metals. It is not possible to unambiguously assign a specific phosphite to a unique resonance.

In the ^{15}N NMR, a doublet is observed at 514.0 ppm ($J_{^{15}N-^{31}P}$ = 6.1 Hz), the nitrido ligand apparently coupling to the phosphite bound to the hinge ruthenium.[26] We propose that structure 6 is most consistent with all the spectroscopic data for $HFeRu_3N(CO)_{10}[P(OCH_3)_3]_2$.

In the anion **5**, the iron atom is found exclusively in the hinge position, while the neutral product 6 contains iron exclusively in the wing-tip position. The identification of intensely colored intermediates as N–H species and their possible role in determining the observed isomeric purity will be discussed below.

CO Trapping Experiments. In each of the protonation reactions, an unstable, dark intermediate was formed before the metal hydride was isolated. Information regarding the identity of these intermediates was obtained from trapping experiments. Conducting the protonation reactions under a CO atmosphere resulted in a dramatic reduction in the lifetimes of the intensely colored intermediates, as well as the isolation of new trinuclear imido (NH) clusters.

When the protonation of $[FeRu_3N(CO)_{12}]^{1-}$ is run in the presence of excess CO, four products are isolated. The major product of the protonation in the absence of CO, $HFeRu_3N(CO)_{12}$, is only isolated in 15% yield from a CO-saturated solution. The previously characterized anion, $[FeRu_4N(CO)_{14}]^{1-}$,[6] is formed in 11% crystallized yield. The major product (45% yield) of the protonation, a new imido cluster $FeRu_2(NH)(CO)_{10}$, **7**, can be chromatgraphically separated from trace amounts of a second new imido cluster $Ru_3(NH)(CO)_{10}$, **8**, which will be discussed below.

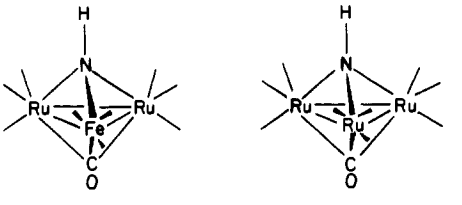

7 **8**

Unique features of the infrared spectrum of $FeRu_2(NH)(CO)_{10}$ include a sharp carbonyl stretch at 1743 cm^{-1} and a very weak N–H stretching absorption at 3372 cm^{-1}. The proton NMR provides further evidence of an N–H functional group, as a triplet is observed at 6.58 ppm ($J_{^1H-^{14}N}$ = 54 Hz). In the mass spectrum, loss of 10 carbonyl units from the parent ion at 555 can be seen. We propose the structure of $FeRu_2(NH)(CO)_{10}$ (**7**) to be similar to other structurally characterized $M_3(\mu_3\text{-}NR)(\mu_3\text{-}CO)(CO)_9$ clusters, such as $Ru_3(NOMe)(CO)_{10}$,[21] $Fe_3(NSiMe_3)(CO)_{10}$,[20] and $Ru_3(NPh)(CO)_{10}$.[23]

Similar chemistry is observed during the protonation of $[Ru_4N(CO)_{12}]^{1-}$. An intense, purple solution formed by the addition of acid reacts within 10 min with CO to produce trace amounts of $HRu_4N(CO)_{12}$, $[Ru_5N(CO)_{14}]^{1-}$, and a new cluster $Ru_3(NH)(CO)_{10}$, **8**. The imido proton resonated at 5.7 ppm ($J_{^1H-^{14}N}$ = 54 Hz) in the proton NMR spectrum, while the N–H stretching frequency is 3378 cm^{-1}. A triply bridging CO stretch occurs at 1749 cm^{-1} in the infrared spectrum. The terminal carbonyl region indicates a highly symmetrical geometry and is virtually superimposable with that of the structurally characterized $Ru_3(NPh)(CO)_{10}$.[23] We, therefore, propose the structure shown above for $Ru_3(NH)(CO)_{10}$, **8**.

Since neither the anionic starting clusters nor the $HM_4N(CO)_{12}$ products react with CO under these mild conditions and since the lifetime of the colored intermediate is reduced, it can be concluded that the CO is reacting with an intermediate to form the imido products. The isolation of N–H-containing products suggests that the intermediates also contain N–H ligands. A possible rationale outlining these reactions is given in eq 4–8.

$$[Ru_4N(CO)_{12}]^{1-} + CF_3SO_3H \rightleftharpoons Ru_4(NH)(CO)_{12} + CF_3SO_3^{1-} \quad (4)$$

$$Ru_4(NH)(CO)_{12} + 3CO \rightarrow Ru_3(NH)(CO)_{10} + Ru(CO)_5 \quad (5)$$

$$Ru_4(NH)(CO)_{12} \rightarrow HRu_4N(CO)_{12} \quad (6)$$

$$[Ru_4N(CO)_{12}]^{1-} + Ru(CO)_5 \rightarrow [Ru_5N(CO)_{14}]^{1-} + 3CO \quad (7)$$

$$3Ru(CO)_5 \rightarrow Ru_3(CO)_{12} + 3CO \quad (8)$$

(25) As the temperature is raised, the broad peak from the iron tricarbonyl group gradually sharpens until it reaches the fast-exchange limit at ~−10 °C. When the temperature is raised from −95 to −70 °C, the peaks at 199.0 and 190.6 ppm, due to carbonyls c and d, begin to broaden. The spinning tricarbonyl exchange process predicts that the resonance at 199.0 ppm (d) will broaden faster than the resonance at 190.6 ppm (c), since the former exchange is every process whereas the latter only one in two. This is observed; at −40 °C the resonance due to carbonyl d has collapsed into the base line and that due to c is still observable. The 25 °C spectrum shows the peak due to c and d beginning to grow in at ~193 ppm. Also, peaks e, f, and g from the two-hinge ruthenium tricarbonyls are just beginning to broaden. As the temperature is raised to 100 °C, the peak due to carbonyls c and d continues to grow in at 192.9 ppm and reaches the fast-exchange limit at 100 °C. The resonances at 186.0 (e) and at 195.0 ppm (f and g) continue to broaden and are collapsed into the base line at 100 °C, the highest temperature measured.

(26) Out of the five compounds having the general formula $[HFeRu_3N(CO)_{12-n}[P(OCH_3)_3]_n$, n = 1–3 (two isomers for n = 1, two isomers for n = 2, and one structure for n = 3) $^{15}N-^{31}P$ coupling is observed only when there is a $J_{^1H-^{31}P}$ of 8–9 Hz. We interpret this to mean that $^{15}N-^{31}P$ coupling is observable only when the phosphite is bound to a hinge ruthenium atom.[7]

As only small amounts of $HM_4N(CO)_{12}$ are isolated in the presence of CO, eq 6 must be slow relative to fragmentation (eq 5). We have independently shown that eq 7 occurs at room temperature.[5] Alternatively, $Ru(CO)_5$ may react directly with $Ru_4(NH)(CO)_{12}$ to give $HRu_5N(CO)_{14}$, which could deprotonate forming $[Ru_5N(CO)_{14}]^{1-}$.

A third new imido cluster is obtained from the protonation of $\{FeRu_3N(CO)_{10}[P(OCH_3)_3]_2\}^{1-}$ in the presence of CO. Reaction of the dark-green intermediate with CO is complete within 20 min, to yield $HFeRu_3N(CO)_{10}[P(OCH_3)_3]_2$, 6, in trace amounts, an as yet unidentified anionic cluster, and $FeRu_2(NH)(CO)_9[P(OCH_3)_3]$, **9**, as the major product (41% yield). The imido stretching frequency of **9** is 3374 cm^{-1}, and a triplet at 6.7 ppm ($J_{^1H-^{14}N}$ = 43 Hz) is assigned to the imido proton, a downfield shift of only 0.2 ppm from the unsubstituted analogue, $FeRu_2(NH)(CO)_{10}$, **7**. An unusual feature in the infrared spectrum is observed in the triply bridging CO stretching region. Phosphite substitution caused the sharp peak at 1743 cm^{-1} found in $FeRu_2(NH)(CO)_{10}$ to decrease in intensity and to resolve into two peaks separated by 10 cm^{-1} at 1725 and 1715 cm^{-1}. The two narrowly spaced peaks must be attributed to the presence of two isomers in solution. To resolve the structural ambiguities, an X-ray structural analysis of $FeRu_2(NH)(CO)_9[P(OCH_3)_3]$ (**9**) was undertaken, as discussed above, and it was found to have the structure shown in Figure 2. The phosphite was located on a ruthenium atom, in the symmetric position trans to the NH ligand, and the triply bridging carbonyl is symmetrically bound to all three metal atoms. One plausible explanation for the structural isomer would involve the rotation of the $Ru(CO)_2[P(OCH_3)_3]$ group so that the phosphite is in one of the two cis positions relative to the NH.

Characterization of $M_4(NH)L_{12}$. None of the intermediates formed during the protonations of any of the nitrido anions could be isolated as a solid. The lifetimes of these intermediates increased in the order $[FeRu_3N(CO)_{12}]^{1-} \ll [Ru_4N(CO)_{12}]^{1-} < \{FeRu_3N(CO)_{10}[P(OCH_3)_3]_2\}^{1-}$. The study of the bis(phosphite)-substituted cluster was particularly valuable because its intermediate was long-lived and present in large enough quantity to allow spectroscopic characterization.

As discussed above, the product hydride, 6, exists in only one isomeric form, which has undergone a substantial cluster framework rearrangement. Such product specificity is not inherent to the system; the thermal reaction of $P(OCH_3)_3$ with $HFeRu_3N(CO)_{12}$ produces two disubstituted isomers. One is structure 6, while the predominant isomer contains both $P(OCH_3)_3$ ligands on the wing-tip metals (one Fe and one Ru), **10**.[6] The regios-

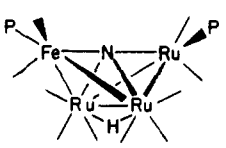

10

pecificity of the rearrangement occurring during the protonation reaction, coupled with spectroscopic information, has allowed a reasonably detailed sequence of events of be proposed.

When ^{15}N-enriched **5** is protonated, the ^1H NMR spectrum exhibits two resonances that can be attributed to N-H groups (no metal hydride resonances were observed). At +15.7 ppm, a doublet of triplets is observed with $J_{^1H-^{15}N}$ = 76.9 and $J_{^1H-^{31}P}$ = 11.2 Hz. The second resonance is located at 5.79 ppm ($J_{^1H-^{15}N}$ = 72.3 Hz) in the region most similar to other clusters containing the μ_3-NH ligand. Table IX lists the proton chemical shifts for a series of known carbonyl clusters containing imido ligands.[15,27-30] While these shifts do exhibit a dependence on the three metals

Table IX. Spectroscopic Properties of μ_3-NH Ligands in $M_3(\mu_3\text{-NH})L_{10}$ Clusters

compound	ν_{N-H}, cm^{-1} (CH_2Cl_2)	δ ^1H, ppm ($CDCl_3$)	ref
$FeCo_2(NH)(CO)_9$	3357	10.6	27
$Fe_3(NH)(CO)_{10}$	3350	9.5	15
$FeRu_2(NH)(CO)_{10}$	3372	6.5	this work
$FeRu_2(NH)(CO)_9[P(OCH_3)_3]$	3374	6.7	this work
$Ru_3(NH)(CO)_{10}$	3378	5.7	this work

bridged by the NH ligand, the unusual nature of the +15.7 ppm resonance is clearly apparent. The upfield peak at +5.79 ppm fits into the "normal" region for a μ_3-NH ligand and most closely matches the position of $Ru_3(NH)(CO)_{10}$. When this experiment is conducted with the ^{14}N-containing cluster, two broad triplets are observed at +15.2 ppm ($J_{^1H-^{14}N}$ = 53 Hz) and +5.8 ppm ($J_{^1H-^{14}N}$ = 43 Hz).

The ^{15}N NMR spectrum of the dark-green solution exhibits two resonances: one doublet located at 283 ppm ($J_{^{15}N-^1H}$ = 76.9 Hz) and the second doublet located at 91 ppm ($J_{^{15}N-^1H}$ = 72.3 Hz) in a ~2:1 intensity ratio, respectively. Both the relative abundance and the coupling constants indicate that the isomer with the unusual proton resonance gives rise to the downfield ^{15}N resonance. As in the discussion on the ^1H chemical shifts, the 283 ppm resonance is in an unusual position for an NH ligand. While fewer data are available on ^{15}N shifts, a value of 82.5 ppm with a $J_{^{15}N-^1H}$ = 77.5 Hz has been reported for $H_2Ru_3(NH)(CO)_9$.[29] The relative abundance of the two ^{15}N resonances remains constant with time as they decrease in intensity and the intensity of the absorption due to $HFeRu_3N(CO)_{10}[P(OCH_3)_3]_2$ increases. No other nitrogen resonances were visible in this reaction.

Further information about the dark-green intermediate was obtained from the infrared spectrum. Although the complexity of the terminal carbonyl region does not lend itself to interpretation, the N-H stretching region could be easily monitored during protonation. Immediately following addition of the acid, two weak peaks of equal intensity can be observed at 3336 and 3273 cm^{-1}. After 5 min, the relative height of the peak at 3273 cm^{-1} has decreased but from this point on the relative intensities of the two peaks remains constant as they slowly disappear.

These data allow us to make reasonable assignments of the structures of these two isomers. First of all, the formula, $FeRu_3(NH)(CO)_{10}[P(OCH_3)_3]_2$, has a 60-electron count, which is most commonly found in closed tetrahedral clusters. The spectral data indicate that one of the NH groups acts as a triply bridging ligand. A species similar to the structurally characterized compound, $Os_4(NCH_3)(CO)_{12}$,[31] **11**, would appear to be the most likely candidate. The tetrahedron comprised of one $Fe(CO)_3$, one

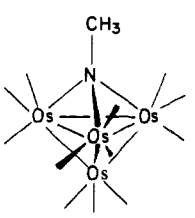

11

$Ru(CO)_3$, and two $Ru(CO)_2[P(OCH_3)_3]$ apices would have three unique M_3 faces, yet only one μ_3-NH resonance is observed. As mentioned above, the δ ^1H of the N-H ligand is characterisitically dependent on the nature of the three metals it bridges. The comparison between $FeRu_2(NH)(CO)_{10}$ and $FeRu_2(NH)(CO)_9[P(OCH_3)_3]$ illustrates that the substitution of a $P(OCH_3)_3$ for a CO has little effect on the δ ^1H of the N-H ligand. The spectrum of $FeRu_2(NH)(CO)_9[P(OCH_3)_3]$ further shows no resolvable H-P coupling, a feature also absent from the spectrum of the μ_3-NH ligand of the intermediate. Since the δ ^1H of 5.79 ppm is closer to the value for $Ru_3(NH)(CO)_{10}$, we suggest that

(27) Fjare, D. E.; Keyes, D. G.; Gladfelter, W. L. *J. Organomet. Chem.* **1983**, *250*, 383.
(28) Johnson, B. F. G.; Lewis, J.; Mace, J. M. *J. Chem. Soc., Chem. Commun.* **1984**, 186.
(29) Smieja, J. A.; Stevens, R. E.; Fjare, D. E.; Gladfelter, W. L. *Inorg. Chem.* **1985**, *24*, 3206.
(30) Smieja, J. A.; Gladfelter, W. L. *J. Organomet. Chem.* **1985**, *297*, 349.
(31) Lin, Y. C.; Knobler, C. B.; Kaesz, H. D. *J. Organomet. Chem.* **1981**, *1981*, C41.

Scheme I

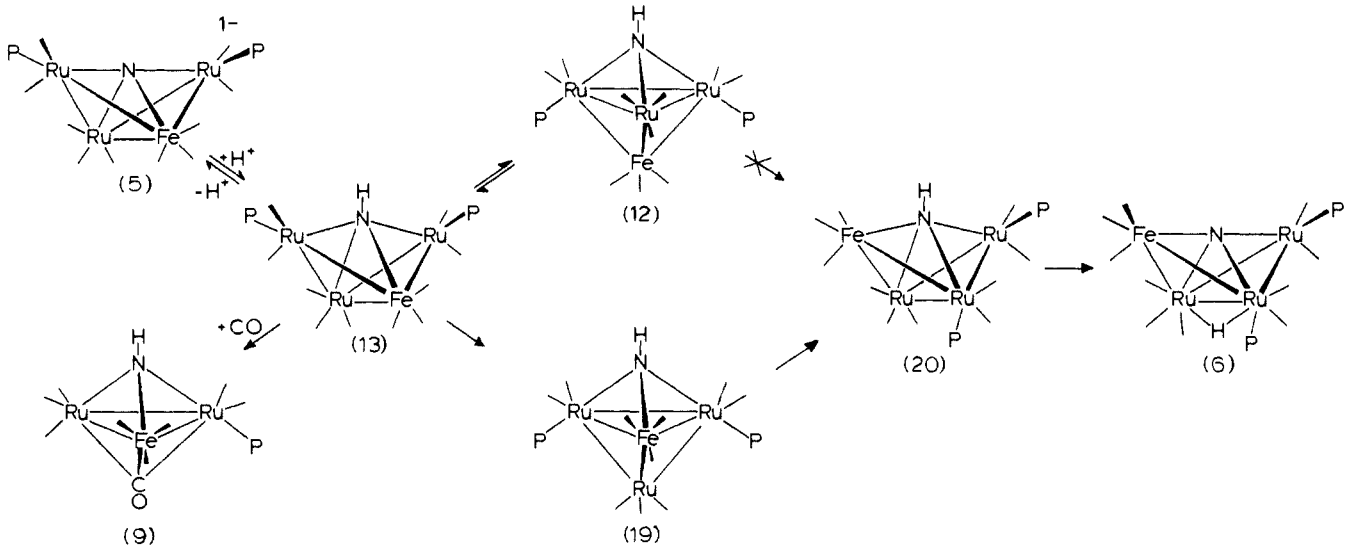

structure **12** (Scheme I) is the most likely candidate containing the μ_3-NH ligand.

The second isomer has several unusual properties that make it unlikely to contain a μ_3-NH ligand. Both the ^1H and ^{15}N shifts are far downfield from the characteristic μ_3-NH region. Also, the intense color is most likely associated with this isomer since **12** is formally saturated and is unlikely to have an unusual color. We suggest that the above data can be reconciled with a bufferfly metal core with the N–H ligand bridging all four metal atoms, **13**. A second possible structure, **14**, similar to $HFe_4(CH)(CO)_{12}$,[32]

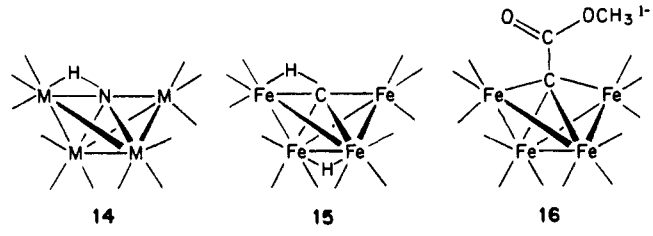

14 **15** **16**

15, can be ruled out on the basis of the ^1H NMR data. The interaction of the hydrogen of the η^2-C–H ligand with the metal has the effect of moving the δ ^1H up to −5.93 ppm. This trend is opposite that found in the μ_4-NH ligand.

As drawn, **13** would fit into a class of compounds prepared by Bradley and co-workers[33] that contain a butterfly metal geometry with only 60 cluster electrons. $[Fe_4(CCO_2CH_3)(CO)_{12}]^{1-}$, **16**, was the first example of this group of compounds and can be considered as an electron-deficient cluster. Alternatively, it has been pointed out[34] that the use of the cluster electron pair counting rules correctly predicts the trigonal-bipyramidal structure of $[Fe_4(CCO_2CH_3)(CO)_{12}]^{1-}$ when the carbon is considered as a cluster vertex. Along this same line, both isomers of $FeRu_3(NH)(CO)_{10}[P(OCH_3)_3]_2$, **12** and **13**, can be considered as trigonal-bipyramidal clusters, with the NH occupying an apex site. In the structure with the μ_3-NH, **12**, an axial apex is occupied, while in **13** the μ_4-NH occupies an equatorial site. The coupling of the imido hydrogen to both phosphite ligands means that the two $Ru(CO)_2[P(OCH_3)_3]$ groups must be equivalent. Structure **13** (Scheme I), in which these groups both occupy axial sites of the trigonal bipyramid, is the most reasonable arrangement. This isomer has the same geometry as found in the starting anion, $\{FeRu_3N(CO)_{10}[P(OCH_3)_3]_2\}^{1-}$.

The last point to consider regarding the two isomers of $FeRu_3(NH)(CO)_{10}[P(OCH_3)_3]_2$ is that they appear to be in equilibrium with each other. Once the isomer ratio is established following the protonation, it remains constant as conversion proceeds to $HFeRu_3N(CO)_{10}[P(OCH_3)_3]_2$. Little is known about the rearrangements of the apex groups in this type of cluster.

In two related compounds, two isomeric forms of $[HFe_4(CO)_{13}]^{1-}$ [35,36] and $[Fe_4(AuPEt_3)(CO)_{13}]^{1-}$ [37] have been observed spectroscopically and found to interconvert. It was suggested that one isomer contained a butterfly arrangement of iron atoms, while the second existed as a closed tetrahedron of irons. Further evidence of such a rearrangement comes from the reaction used to prepare $[Fe_4(CCH_3)(CO)_{12}]^{1-}$, **17**, eq 9.[38] Also, in a recent

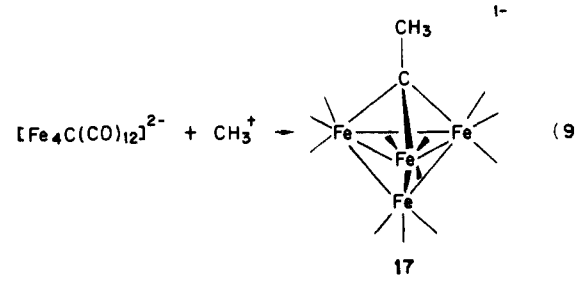

17

study of $[FeRu_3N(CO)_{12}]^{1-}$,[6] we did directly observe a rearrangement of the metals within the butterfly core. The process of converting **13** to **12** can occur very simply by moving the N–H ligand away from the reader (breaking the Fe–N bond), while folding the two wings of the butterfly cluster toward one another (making the Ru–Ru bond).

Mechanism of the Reaction. Having established that **12** and **13** are reasonable structures for the two N–H isomers, we now continue with the discussion of Scheme I. At this stage, recall that the mechanism must explain the regiospecificity obtained in the final product, **6**. In this structure, the "open" M–M bond of the butterfly is an Fe–Ru bond. It is clear from an examination of the structures of the observed intermediate that there is no simple, one-step process leading directly to **6**. The N–H-containing structure **20** is the likely precursor to the final nitrido product. A route from **13** to **20** can be envisioned by simply twice repeating a rearrangement analogous to the interconversion between **13** and **12**. If the N–H ligand in **13** is moved out toward the reader as the cluster closes, a Ru–N bond would be broken as the Ru–Ru

(32) Tachikawa, M.; Muetterties, E. L. *J. Am. Chem.* **1980**, *102*, 4541.
(33) Bradley, J. S.; Ansell, G. B.; Hill, E. W. *J. Am. Chem. Soc.* **1979**, *101*, 7417.
(34) Bradley, J. S.; Ansell, G. B.; Leonowicz, M. E.; Hill, E. W. *J. Am. Chem. Soc.* **1981**, *103*, 4968.
(35) Manassero, M.; Sansoni, J.; Longoni, G. *J. Chem. Soc., Chem. Commun.* **1976**, 919.
(36) Horwitz, C. P.; Shriver, D. F. *Organometallics* **1984**, *3*, 756.
(37) Horwitz, C. P.; Holt, E. M.; Shriver, D. F. *J. Am. Chem. Soc.* **1985**, *107*, 281.
(38) Holt, E. M.; Whitmire, K. H.; Shriver, D. F. *J. Am. Chem. Soc.* **1982**, *104*, 5621.

bond is formed. The product of this conversion, **19**, contains a μ_3-NH ligand bridging an $FeRu_2$ face. By reinsertion into either one of the equivalent Fe–Ru bonds, **19** is converted directly into **20**. Note that these steps not only allow us to obtain a product with the N inserted into a Fe–Ru bond, but they also predict the correct relative positions of the $Ru(CO)_3$ and two $Ru(CO)_2[P(OCH_3)_3]$ groups.

It is reasonable that the last step in the process, the migration of the hydrogen from the nitrogen to the hinge M–M bond, would first involve a bridge between the N and the wing-tip metal, such as depicted in **14**. The next step in the route would involve a shift to the structure shown in **18**, followed by the final migration to the hinge M–M bond. The existence of one structurally characterized butterfly nitrido cluster that does contain a hydrogen bridging a wing-tip to the hinge M–M bond[16] supports the viability of **18** as an intermediate. Perhaps the most important precedent for the N–H to M–H conversion is the fluxional process observed in $HFe_4(CH)(CO)_{12}$, **15**. Using spin saturation transfer techniques, the two hydrogens were found to undergo *intramolecular* exchange.[32]

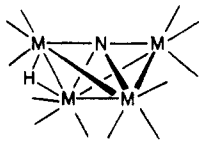

18

In the homonuclear cluster, $[Ru_4N(CO)_{12}]^{1-}$, there is no need for such an elaborate scheme to describe the mechanism of product formation. Proton migration can occur from the intermediate, $Ru_4(NH)(CO)_{12}$, directly to the neutral nitrido product. For $[FeRu_3N(CO)_{12}]^{1-}$, the predominant isomer in solution contains the iron in the wing-tip position[6] and therefore requires no rearrangement of the metals upon protonation to yield $HFeRu_3N(CO)_{12}$. Once the isomer with the Fe in the hinge position is protonated, it would have to proceed in a path similar to that described for $\{FeRu_3N(CO)_{10}[P(OCH_3)_3]_2\}^{1-}$ before reaching the correct form of the product.

In the three anions studied, there are only three different ML_3 groups: $Fe(CO)_3$, $Ru(CO)_3$, and $Ru(CO)_2[P(OCH_3)_3]$. To eq 1–3, we can add the results of the study of $[Fe_4N(CO)_{12}]^{1-}$ which rapidly protonates directly to $HFe_4N(CO)_{12}$ even at low temperatures under CO (i.e., too fast to observe or even trap any intermediates). From these studies, we infer that the rate of conversion from the imido intermediate to the final hydrido product is dependent on the nature of the wing-tip ML_3 group, with the rate decreasing in the order $Fe(CO)_3 > Ru(CO)_3 > Ru(CO)_2[P(OCH_3)_3]$.

Acknowledgment. We gratefully acknowledge the National Science Foundation for supporting this research.

Registry No. 1, 84549-71-3; **2**, 90968-69-7; **3**, 100927-51-3; **4**, 76791-95-2; **5**-PPN, 100927-53-5; **5**-Et_4N, 100927-57-9; **6**, 100938-64-5; **7**, 100927-54-6; **8**, 100938-65-6; **9**, 100938-66-7; **12**, 100938-67-8; **13**, 100927-55-7; $Ru_3(CO)_{12}$, 15243-33-1; $PPN[FeRu_4N(CO)_{14}]$, 90990-44-6; $PPN[Ru_4N(CO)_{12}]$, 92845-78-8; $PPN[Ru_5N(CO)_{14}]$, 83312-28-1; $HFeRu_3N(CO)_{11}[P(OCH_3)_3]$, 100927-56-8; Fe, 7439-89-6; Ru, 7440-18-8.

Supplementary Material Available: A listing of the structure factors and thermal parameters for both of the structures (15 pages). Ordering information can be found on any current masthead page.

Epoxidation of Olefins with Cationic (salen)Mn^{III} Complexes. The Modulation of Catalytic Activity by Substituents

K. Srinivasan, P. Michaud, and J. K. Kochi*

Contribution from the Department of Chemistry, University of Houston, University Park, Houston, Texas 77004. *Received August 28, 1985*

Abstract: Cationic manganese(III) complexes of the salen ligand [*N*,*N*′-ethylenebis(salicylideneaminato)] are effective catalysts for the epoxidation of various olefins with iodosylbenzene as the terminal oxidant. The presence of electron-withdrawing groups, such as 5,5′-dichloro or -dinitro substituents, enhances the catalytic activity of the (salen)Mn^{III} catalyst in measure with the electron-deficient character of the cationic complex as evaluated by the standard reduction potential $E°$. Various types of olefins, including substituted styrenes, stilbenes, and cyclic and acyclic alkenes, are epoxidized in 50–75% yields within 15 min at ambient temperatures in acetonitrile. Stereospecific epoxidation is achieved with *trans*-olefins such as (*E*)-2-hexene and (*E*)-β-methylstyrene. *cis*-Olefins produce high yields of *cis*-epoxides which contain minor amounts of the corresponding trans isomer. Competition from allylic oxidation is minor with this catalyst system—cyclohexene being converted selectively to its epoxide accompanied by only traces of cyclohexenol. Competition studies indicate that the relative reactivity of olefins toward catalytic epoxidation with the cationic (salen)Mn^{III} complexes falls into an unusually narrow range, the difference between the most reactive, *p*-methoxystyrene, and the least reactive, 1-octene, being only a factor of 10. The effect of donor ligands such as pyridine and imidazole is discussed in the context of a radical-like behavior of an oxomanganese species as the reactive intermediate. The latter is supported by some preliminary studies of alkane oxidation using cyclohexane as a model.

Metal catalysis of the oxidation of various organic substrates is of synthetic as well as of biochemical interest.[1] In our earlier study of the chromium-catalyzed epoxidation of olefins, we showed how oxochromium(V) species play a critical role in the catalytic cycle.[2,3] The successful isolation and determination of the X-ray crystal structure of the reactive oxochromium(V) intermediates were allowed by the use of the salen [*N*,*N*′-ethylenebis(salicylideneaminato)] ligand. Indeed as a ligand, salen has the desirable characteristic of being readily subject to systematic modification of its electronic and steric properties. In particular, substituents on the 5-positions which are para to the pair of ligating oxygen atoms strongly perturb the redox properties of (salen)metal

(1) Sheldon, R. A.; Kochi, J. K. "Metal-Catalyzed Oxidations of Organic Compounds"; Academic: New York, 1981.

(2) Siddall, T. L.; Miyaura, N.; Huffman, J. C.; Kochi, J. K. *J. Chem. Soc., Chem. Commun.* **1983**, 1185.

(3) Samsel, E. G.; Srinivasan, K.; Kochi, J. K. *J. Am. Chem. Soc.* **1985**, *107*, 7606.

0002-7863/86/1508-2309$01.50/0